CHARACTERIZATION OF DYNAMIC FRACTURE IN COPPER UNDER UNIAXIAL STRESS AND UNIAXIAL STRAIN

A. Zurek, J. Johnson, C. Frantz

JOURNAL DE PHYSIQUE
Colloque C3, Supplément au n°9, Tome 49, septembre 1988

CHARACTERIZATION OF DYNAMIC FRACTURE IN COPPER UNDER UNIAXIAL STRESS AND UNIAXIAL STRAIN

A.K. ZUREK, J.N. JOHNSON and C.E. FRANTZ

Los Alamos National Laboratory, Los Alamos, NM 87545, U.S.A.

RÉSUMÉ - Nous avons caractérisé les modes de rupture dans le cuivre lors d'une tension uniaxiale dynamique (essais aux anneaux étendants) et d'une déformation uniaxiale dynamique (essais d'éclat). On a mesuré la résistance à éclatement dans le cuivre en fonction de la taille des grains, de la pureté et de la porosité initiale. On a développé un modèle unifié pour la rupture ductile, et on présente une prévision qualitative des magnitudes relatives de la porosité et de la déformation due à la déformation plastique pour des essais d'éclat et des essais à la traction uniaxiale.

ABSTRACT - We have characterized fracture modes in copper under conditions of dynamic uniaxial tension (expanding ring tests) and dynamic uniaxial strain (spall tests). The spall strength in copper was measured as a function of grain size, purity and initial porosity. A unified model for ductile fracture is developed, and a qualitative prediction of the relative magnitudes of porosity and plastic deformational strain for spall and uniaxial tension tests is presented.

1. INTRODUCTION

In this paper two specific dynamic fracture processes will be discussed: tensile fracture under dynamic uniaxial stress conditions (expanding ring) and spallation under dynamic uniaxial strain. Catastrophic failure in an expanding ring is preceded by a large amount of homogeneous plastic strain and little void growth until the latter stages of necking, where void growth and coalescence are responsible for material separation. In a spallation test void nucleation and growth dominate the tensile plastic flow process from the very beginning. The reason for this observed difference has to do with the extremely different tensile stress states in the two cases.

Under conditions of uniaxial loading in the case of a notched or smooth specimen, voids are subject to a nearly uniaxial tensile stress field; homogeneous plastic strain dominates the flow process in the early stages. Fracture data are usually analyzed with the assumption that the void growth (volumetric plasticity) is nonexistent [1,2]. Under conditions of dynamic uniaxial strain (spallation test) the principal stress components differ by the flow stress Y, and thus voids are subject to a nearly isotropic tensile stress field; void growth dominates all stages of the fracture process [3,4]. In descriptions of spallation, porosity serves as a variable to describe the threshold for void growth as well as the fracture criterion.

In this work we present scanning electron micrographs of fracture surfaces of copper in the two cases, experimental data on spall strength as a function of grain size and impurity content, and some theoretical considerations which allow a unified treatment of ductile fracture under a wide range of combined tensile - shear stress states.

2. MATERIALS AND EXPERIMENTAL PROCEDURE

The expanding ring experiments were performed by a team led by W. H. Gourdin at Lawrence Livermore National Laboratory. The material used was OFHC copper, annealed to give 10 μm and 150-200 μm average grain sizes. The specially prepared ring specimens, 1 mm^2 in cross section [5], were launched electromagnetically [6]. Induced electrical currents in the specimens resulted in a temperature increase of approximately 150°C. Dynamic stress-strain data were obtained by measuring expansion speed using VISAR instrumentation [6]. The strain rate in an individual test varied from 10^3 s^{-1} to 10^4 s^{-1}. Fracture surfaces of necked regions were examined using scanning electron microscopy.

The spall tests were performed on OFHC and ETP copper samples, annealed to give average grain sizes of 40 and 200 μm. The specimens were subjected to planar impact in a 40 mm gas gun. The specimen and flyer plate geometries and dimensions are given elsewhere [7]. All specimens were impacted with a flat flyer at velocities of approximately 425 m/s, producing a shock wave of 8 GPa pressure and 1 μs duration. Impacted specimens were recovered using a specially designed soft recovery catcher tank to ensure minimal damage to fracture surfaces [8]. In each test, impact pressure and spall strength were measured using manganin gauges pulsed by Wheatstone bridge circuits in conjunction with a delayed triggering system to ensure a high signal-to-noise ratio. Recovered samples, with spall fracture surfaces intact, were examined by stereo-scanning electron microscopy.

3. RESULTS

Figures 1 a and b show the typical fracture surfaces of the electromagnetically expanded copper rings with an average 10 and 150 μm grain size, respectively. The number of fragments generated in the process does not vary strongly with grain size [6], but is dependent on the distribution of random physical imperfections (inclusions, the burrs from sample machining, e.t.c.) which serve as nuclei for failure. In our observations, however, we have found the final cross sectional area of the necked region to be dependent on the grain size. The smaller grain size material fails with the larger cross sectional fracture area than the large grain size material (compare the typical cross sectional area of fracture surface in Fig. 1a to b). For 10 μm grain size sample the neck fracture area is approximately 150 μm on a side, while in 150 μm samples it is only 60 μm. In the smaller grain size samples there are more void nucleation sites which evolved into ductile dimples than found in the large grain size rings. However, the nucleated sites cover only small fraction (a few percent) of the initial cross sectional area of the sample and are located only in the immediate vicinity of the fracture surface.

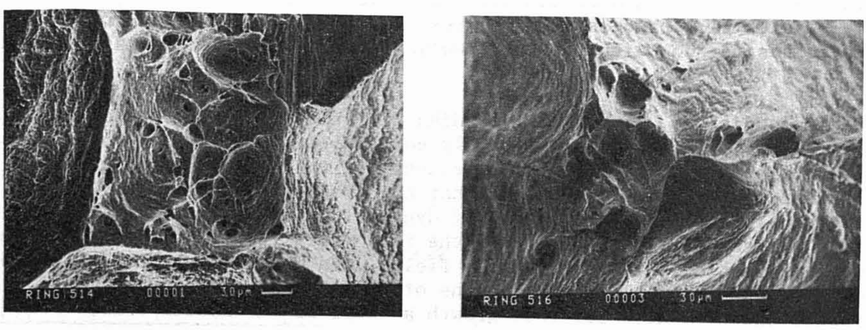

a b

Fig. 1. Expanding ring fracture surfaces in OFHC copper: (a) 10 μm grain size, (b) 150 μm grain size.

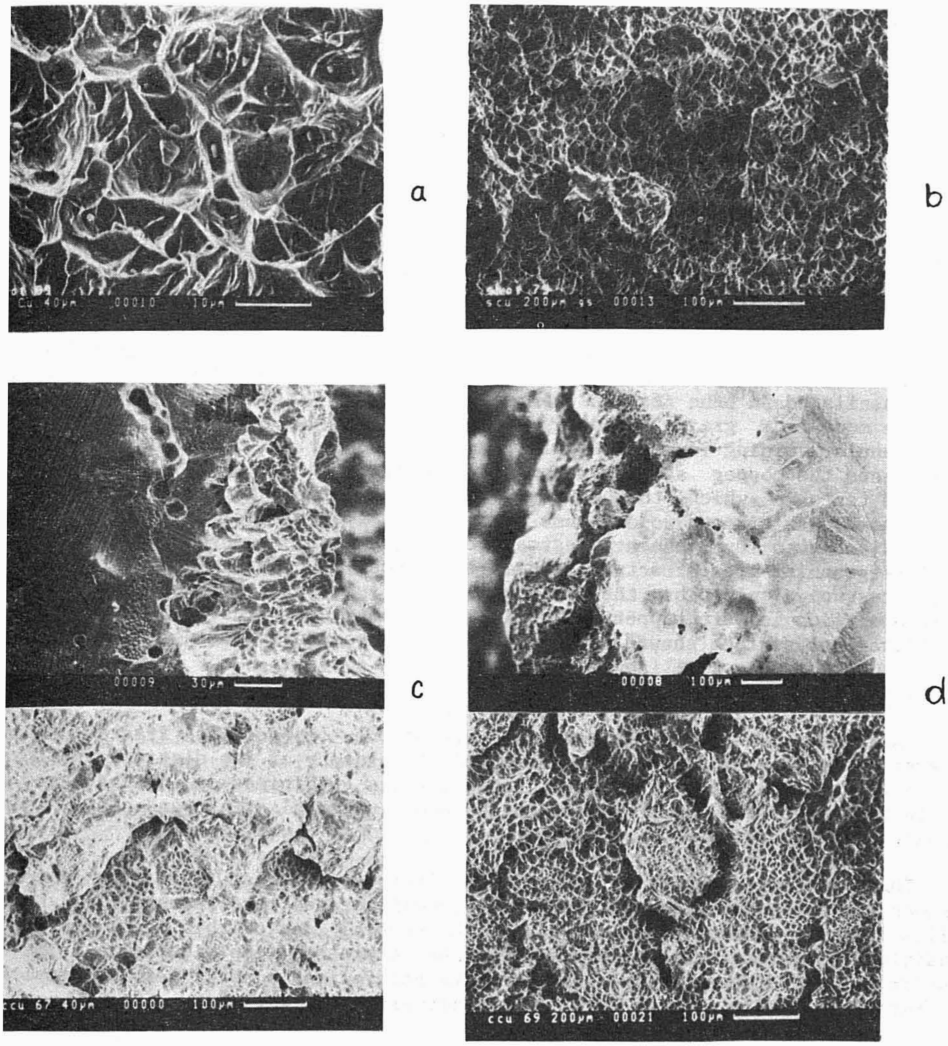

Fig. 2. Spall fracture surfaces: ETP copper (a) 40 µm grain size, -1.5 GPa spall strength, (b) 200 µm grain size, -0.4 GPa spall strength; OFHC copper (c) 40 µm grain size, -2.4 GPa spall strength, (d) 200 µm grain size, -1.5 GPa spall strength. Note: no grain boundary fracture in ETP copper; see low magnification micrograph (b). (c) and (d) show normal view (lower micrographs) and cross-sectional view (top micrographs) with predominant grain boundary fracture mode (d) in 200 µm grain size OFHC copper.

The spall fracture surfaces, in contrast to those of the expanded rings, are fully covered with void nucleation sites and dimples. Figures 2 a through d show spall fracture surfaces observed in our tests, and microstructural differences between them, which we think may account for the range in the measured spall strengths (given in the individual figure captions). We found that the spall strength of the copper varies with its purity and the grain size. The lowest spall strength was found in the ETP 200 µm grain size samples and the highest in the 40 µm grain size OFHC copper [7]. Figures 2 a and b show the fracture surfaces obtained in ETP copper 40 and 200 µm grain size. The inclusion particles in the ETP copper are copper-oxides, which obviously serve as void nucleation sites since almost every dimple has a particle inclusion in the center. In this particular material the spall is void growth controlled, (since void nucleation is not important due to the existing particles in the materials structure), and the differences in the spall strength are due to the differences in the grain size. What appears to be homogeneously nucleated transgranular spall fracture can be found in OFHC small (40 µm) grain size copper, Fig. 2 c. The voids most likely nucleate on the cross slip planes of the edge dislocations, slipping along the <111> plane of the cube faces [9]. In the case of large (200 µm) grain size OFHC copper, the nucleation occurs predominantly at the grain boundaries, Fig. 2 d. In the case of high purity copper we think that the spall is nucleation controlled. The differences in the spall strength, listed in the figure caption, are most likely due to the change of the fracture mode from grain boundary voiding in large grain size material to transgranular voiding in the smaller grained copper. In the above described experiments the copper samples were void free prior to the spall test. We have also designed tests in which the OFHC 200 µm grain size samples were artificially impregnated with a known void volume fraction, $\phi_o = 0.0015$ prior to the spall test. This was achieved by the heat treatment technique developed by Nieh and Nix [10] for the intergranular creep fracture studies in copper. Unfortunately, this technique introduces voids only along the grain boundaries. There is no technique available to introduce voids in pure copper uniformly throughout the grains. In this test, the spall fracture surface showed predominantly grain boundary voiding, as expected.

4. THE UNIFIED DUCTILE FRACTURE MODEL

There are numerous theoretical descriptions of ductile fracture [3,11,12]. However, they generally tend to be directed toward one of two distinct applications: either (1) quasi-static or dynamic tensile tests (performed on notched or smooth cylindrical specimens) or (2) spallation under uniaxial strain and nearly isotropic tensile stress conditions.

The most successful of the former descriptions is that initially suggested by Hancock and MacKenzie [1], and applied to specific cases more recently by Nash and Cullis [2] and Johnson and Cook [13]. The central idea of this description is that conditions of catastrophic separation can be expressed empirically in terms of the non-dimensional stress variable $-p/\tau$ and the generalized plastic deformational strain γ. The formal definition of these quantities are:

mean stress $$-p = \tau_{kk}/3 \qquad (1)$$

generalized shear stress $$\tau = (3/8\ s_{ij}\ s_{ij})^{1/2} \qquad (2)$$

plastic deformational strain $$\gamma = (2/3\ e^p_{ij}\ e^p_{ij})^{1/2} \qquad (3)$$

where $s_{ij} = \tau_{ij} - (-p)\delta_{ij}$ is the deviatoric stress (τ_{ij} are the stress components) and e^p_{ij} is the plastic deviatoric strain. The condition for fracture is expressed as

$$\gamma_f = \gamma_o + \Delta\gamma \exp(ap/2\tau). \qquad (4)$$

A comparison of the quasi-static data of Nash and Cullis [2] to Equation 4 with $\gamma_o = 0.45$, $\Delta\gamma = 2.81$ and a $=2.98$ is shown in Figure 3 along with the expanding ring fracture data for two grain sizes (10 μm and 150-200μm). The plastic strain components are obtained from the expression

$$\gamma_f = \ln A_o/A_f, \qquad 5$$

where A_o is the initial cross-sectional area and A_f is the cross-sectional area at fracture. The quantity $-p/2\tau$ for an initially smooth bar undergoing fully developed plastic flow is $-p/2\tau = 1/3$ [1,2,14].

It is apparent in Figure 3 that greater ductility is achieved in the expanding ring test. This can be due to the higher rate at which the test was conducted (10^3 -10^4 s^{-1}) and to the higher temperature (≈150°C) produced in the ring due to the induced electric current. The effects of strain rate and temperature as discussed by Johnson and Cook [13] are insufficient to account for the large increase in ductility of the expanding copper rings as shown in Figure 3.

Fracture descriptions for spallation involve the nucleation, growth and coalescence of voids under the application of a nearly isotropic tensile stress state. While this is obviously a very complex problem in its entirety, there are some simple aspects that are useful in discussing the main features of spallation in ductile materials; one of these is the relationship between the tensile mean stress at which voids begin to grow and the porosity ϕ [4,15]:

$$p_t = (2Y/3)\ln\phi \qquad 6$$

where Y is the flow stress. Here we neglected a $(1-\phi)$ factor multiplying $\ln\phi$ in the expression derived by Johnson [4], and have kept the form originally given by Carroll and Holt [15]. Equation 6 gives the threshold for void growth in a spallation experiment. For example, an initial porosity of 0.0003, as determined by post-shot analysis on OFHC copper [11], and a flow stress Y = 0.255 GPa give p_t = -1.4 GPa, the spall stress measured by a manganin pressure gauge in a plexiglas backing plate [7]. Equation 6 provides a qualitative means of relating spall strength to porosity and flow stress.

Where the initial porosity can be estimated easily from the volume fraction of large impurities, Equation 6 is most useful. However, conditions are usually such that in very pure materials the source of initial porosity is not obvious; also, the shock pre-compression of the sample changes the porosity seen by the dynamic tensile state. In the case of OFHC (200 μm grain size) copper with an artificially introduced porosity of 0.0015, Equation 6 with Y=0.255 GPa predicts a spall strength of -1.1 GPa, while the measured value is -0.85 GPa. The discrepancy between our measurement and the calculated value for the spall strength can be attributed to the fact that voids in this experiment are nucleated at grain boundaries only, and the model does not differentiate between modes of void nucleation; it assumes uniform void distribution throughout the grains. This suggests that an additional expression may be needed to describe the nucleation process in pure materials.

If one accepts for the moment that void nucleation in pure materials can be calculated (see, for example, [3]), or that we limit consideration to materials containing impurities, there does exist a very straight-forward means of uniting the ductile fracture descriptions for tensile tests and spallation. This is done by using the Gurson [16] flow surface (in the tensile region) in conjunction with the associated flow law:

$$f(\tau_{ij}) = (2\tau/Y)^2 + 2\phi\cosh(-3p/2Y) - 1 - \phi^2 = 0 \qquad 7$$

$$d\varepsilon^p_{ij} = d\lambda\,\partial f/\partial\tau_{ij}\,, \qquad 8$$

where $d\lambda$ is a scalar multiplier determined by the condition that the stress state remains on the flow surface. For isotropic tensile stress conditions ($\tau = 0$), Equation 7 becomes

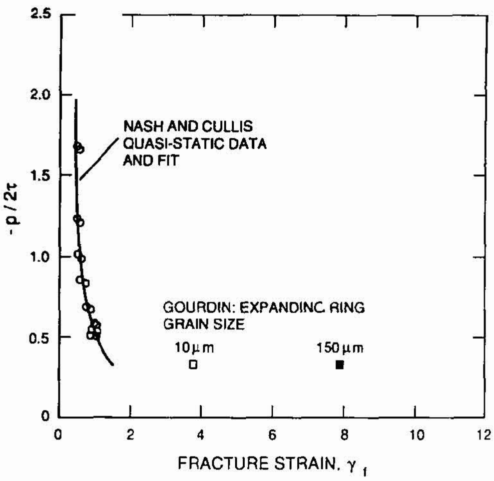

Fig. 3. A comparison of the quasi-static data of Nash and Cullis [2] to Equation 4 and expanding ring fracture data for two grain sizes: 10 μm and 150 μm.

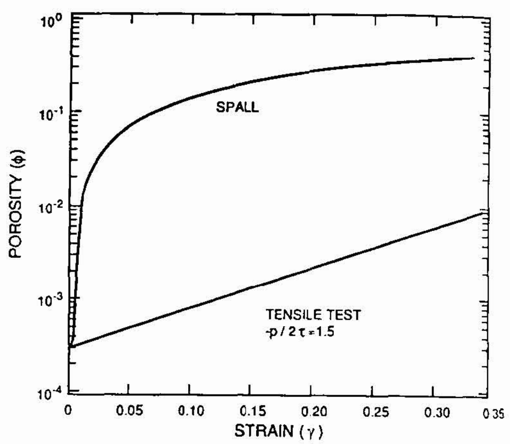

Fig. 4. Plastic deformational strain vs. void growth in a notched tensile bar (uniaxial stress condition) and in a spall experiment (uniaxial strain condition).

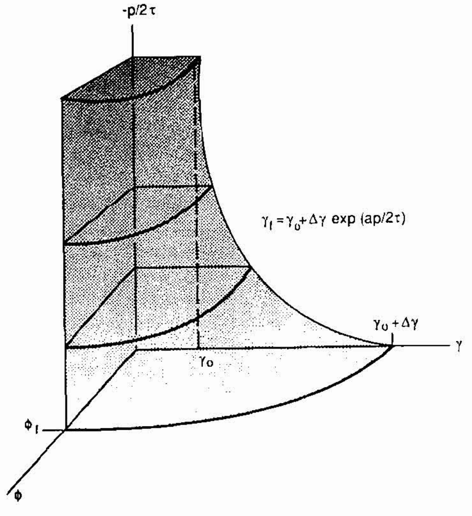

Fig. 5. Fracture surface defined in porosity, deformational strain and stress variable space.

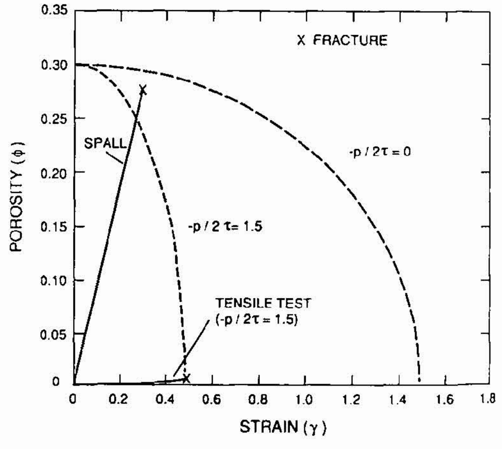

Fig. 6. Strain path for spall and tensile tests shown in Fig. 4. Fracture is indicated by x. Fracture surface at constant $-p/2\tau$ (0 and 1.5) is shown as two broken lines.

$$\cosh(-3p/2Y) = \tfrac{1}{2}\,(\phi + \phi^{-1}) \tag{9}$$

which is exactly equivalent to Equation 6. It can also be shown that the fractional change in void radius in a triaxial stress field is given by (for a fixed number of nucleation sites)

$$dR/R \;=\; \tfrac{1}{2}\,[(1-\phi)Y/2\tau]\; d\gamma \sinh(-3p/2Y). \tag{10}$$

Since the quantity in square brackets above is ≈ 1 (see Eq. 12), we have a good approximation to the Rice and Tracey [17] result:

$$dR/R \approx 0.558\; d\gamma \sinh(-3p/2Y) \tag{11}$$

The Gurson flow surface and associated flow law predict a small change in porosity for a tensile test (expanding ring test as shown in Figure 1). This is because the mean stress $-p$ is small, in which case Equation 7 becomes approximately

$$[2\tau/(1-\phi)Y]^2 - 1 \;=\; 0 \tag{12}$$

which is the von Mises flow surface with reduced flow stress $(1-\phi)Y$. Application of the associated flow law to Equation 12 gives $d\varepsilon^p_{kk} = -d\ln(1-\phi) = 0$.

Equations 7 and 8 can be combined with the stress-strain laws for isotropic and deviatoric deformation, in terms of the bulk and shear moduli B and G for the nonporous solid,

$$d(-p) = (1-\phi)\; B\; [d\ln v \;+\; d\ln(1-\phi)] \tag{13}$$

$$ds_{ij} \;=\; 2(1-\phi)\; G\; (de_{ij} \;-\; de^p_{ij}) \tag{14}$$

to give the stress-strain response of copper (with $\phi_o = 0.0003$) under conditions of uniaxial stress and uniaxial strain, where v is specific volume of the material. The results are shown in Figure 4. The tensile bar calculation shown here is for a notched bar (the ratio of the minimum diameter to the notch radius is 8.85, $-p/2\tau = 1.5$) which produces a slight departure from uniaxial stress conditions at the center of the specimen, and hence greater increase in porosity than would be achieved in a smooth specimen. Nonetheless the tensile bar undergoes far less void growth than the spall experiment.

All that remains to do is to specify when fracture occurs. The condition for fracture in a tensile test is expressed in terms of $-p/\tau$ and γ according to Equation 4. Conditions for fracture in a spall test are expressed in terms of a maximum porosity ϕ_f (in case of copper $\phi_f = 0.30$ [4,11]). One easy generalization of the fracture condition to handle both cases simultaneously is to define a fracture surface (shown in Figure 5) in ϕ, γ, $-p/\tau$ space. The intersection of this surface with the $-p/\tau$, γ plane is given by Equation 4, while the intersection with the $-p/\tau$, ϕ plane is the line $\phi = \phi_f$. The intersection of the fracture surface with the ϕ, γ plane is chosen to be a quarter of an ellipse with ϕ_f and γ_f as the semi-major and semi-minor axes. Figure 6 shows the strain path of Figure 4 in relationship to the fracture surface for copper for two values of $-p/2\tau$ (0 and 1.5): note the linear scale for porosity in Figure 6 and comparison to the logarithmic scale in Figure 4. The conditions of fracture are indicated by a cross at the end of each strain path. Spall fracture is seen to take place under conditions that differ markedly from those occurring in the tensile test. The assumption of constant volume plasticity remains a good approximation in analyses of the tensile test, but is clearly not appropriate in spallation or other fracture modes occurring at large tensile mean stress.

5. SUMMARY

The spall strengths were measured and fracture surfaces compared in copper samples with respect to grain size, impurity content and initial porosity. Fracture in spallation is preceded by a large increase in porosity. Fracture in a tensile test (expanding ring, notched or smooth bar) takes place by means of a few voids that grow and coalesce only in a latter stages of the fracture process. The homogeneous plastic deformation preceding fracture is not accompanied by significant void growth; tensile flow under uniaxial-stress conditions takes place at nearly constant density. Fracture surfaces observed for expanding ring test support that assumption. Finally, we present a unified mathematical model describing plastic flow under conditions of tensile mean stress which, when combined with a generalized fracture surface allows calculation of ductile fracture under a wide variety of tensile/shear loading conditions.

ACKNOWLEDGMENT : This work has been sponsored by the U. S. Air Force Armament Laboratory under Contract No. DE-AI04-79AL 11812 and has been performed under the auspices of the United States Department of Energy.

6. REFERENCES

[1]. Hancock, J. W. and MacKenzie, A. C., J. Mech. Phys. Solids 24 (1976) 147-169.
[2]. Nash, M. A., and Cullis, I. G., "Numerical Modelling of Fracture - A Model for Ductile Fracture in Triaxial States of Stress." 3rd Conference on Mech. Prop. at High Rates of Strain, Oxford Inst. Phys. Conf. Series No. 70 (1984) 307-314.
[3]. Curran, D. R., Seaman, L., and Shockey, D. A., "Dynamic Failure of Solids", Physics Reports 147 (1987) 253-388.
[4]. Johnson, J. N., J. Appl. Phys., 52(4) (1981) 2812-2825.
[5]. Gourdin, W. H., "Metallurgical Effects on the Constitutive and Fragmentation Behavior of OFHC Copper Rings", Proc. of The APS Topical Conference on Shock Wave in Condensed Matter, Monterey, California, July 20-23, 1987.
[6]. Gourdin, W. H., "Electromagnetic Ring Expansion: Experiment, Analysis, and Application to High-Strain-Rate Testing", Proc. of The International Conference on Impact Loading and Dynamic Behavior of Materials, Bremen, FRG, May 18-21, 1987.
[7]. Zurek, A. K., and Frantz, C. E., "Microstructural Aspects of Spallation in Copper", Proc. of The International Conference on Impact Loading and Dynamic Behavior of Materials, Bremen, FRG, May 18-21, 1987.
[8]. Frantz, C. E., and Gray, G. T., "A Water Catch System Inside an Evacuated Catch Tank of a 40 mm Gun System", Proc. of Aeroballistic Range Association Meeting, Quebec, Canada, Sept. 9-12, 1986.
[9]. Stevens, A. L., Davison, L., and Warren, W. E., J. Appl. Phys., 43 (1972) 988.
[10]. Nieh, T. G., and Nix, W. D., Acta Metallurgica 28 (1980) 557-566.
[11]. Seaman, L., Barbee Jr., T. W., and Curran, D. R., Stanford Res. Inst. Tech. Report No. AFWL-TR-71-156, Dec. 1971.
[12]. Meyers, M. A., and Aimone, C. T., Progress in Materials Science 28 (1983) 1-96.
[13]. Johnson, G. R., and Cook, W. H., Eng. Fracture Mechanics 21 (1985) 31-48.
[14]. Bridgman, P. W., Studies in Large Plastic Flow and Fracture, McGraw-Hill, New York, (1952) 11-16.
[15]. Carroll, M. M., and Holt, A. C., J. Appl. Phys. 43 (1972) 1626.
[16]. Gurson, A. L., J. Eng. Materials Tech. 99 (1977) 2.
[17]. Rice, J. R., and Tracey, D. M., J. Mech. Phys. Solids 17 (1969) 201-217.